Study of the Mechanical Characteristics of Sandwich Structures FDM 3D-printed

Rawabe Fatima Faidallah[1], Muammel M. Hanon[2*], Zoltán Szakál[3], István Oldal[3]

[1] Mechanical Engineering Doctoral School, Szent István Campus, MATE University, Páter Károly u. 1, 2100 Gödöllő, Hungary; faidallah.rawabe.fatima.2@phd.uni-mate.hu

[2] Baquba Technical Institute, Middle Technical University (MTU), Muasker Al-Rashid Street, 10074 Baghdad, Iraq; muammel.m.hanon@mtu.edu.iq

[3] Institute of Technology, Szent István Campus, MATE University, Páter Károly u. 1, 2100 Gödöllő, Hungary; szakal.zoltan@uni-mate.hu, oldal.istvan@uni-mate.hu

Abstract: Additive manufacturing (also known as 3D printing) technologies are successfully used in various applications as they offer many advantages in production, such as (i) less material consumption and (ii) shorter manufacturing times, factors that reduce costs. In recent years, experts in 3D printing have focused their studies on designing and printing cellular structures. This structure's advantages (high strength-to-weight ratio, high flexural stiffness-to-weight ratio, high-energy absorption capacity, thermal and acoustical insulation properties) make it widely used in aerospace, sustainable energy, marine, and automotive industries. This study aims to study the mechanical properties of sandwich structures manufactured using polylactic acid (PLA) material with rhombus and honeycomb core shapes as a single part by an FDM 3D printer. First, the functional properties of the sandwich structures were quantified by shape evaluations. Then, tensile, three-point bending, and compression tests were performed to determine the mechanical performance of the different samples. The results show that rhombus structures gave better mechanical behaviour as the tensile, bending, and compression strengths were 15.3%, 39.8%, and 35.1%, respectively, higher than the honeycomb, indicating their reliable core construction.

Keywords: Polylactic acid; 3D printing; Honeycomb core structure; Rhombus structure; Mechanical performance

1 Introduction

Additive manufacturing (AM), alias 3D printing, can be defined as the "process of joining materials to make parts from 3D model data" [1]. Often the products are constructed layer upon layer [1, 2], as opposed to formative and subtractive manufacturing methods. In the AM process, the material is fused, cooled, and solidified, thus obtaining 3D geometries without adopting complex moulds [3]. The product details are taken from a computer-aided design (CAD) file, which is later converted into a stereolithography (STL) file. The model is created in a 3D CAD software (e.g., Solidworks) and is approximated by triangles and cut into slices containing each layer's information to be printed [4]. Nowadays, additive manufacturing is involved in mechanical engineering applications for the research and development of different elements extending from simple constructs employed in daily life up to the complex components in aerospace implementations [5, 6].

Fused deposition modeling (FDM) is one of AM technologies that provides excellent mechanical, chemical, and thermal endurance and has become one of the most widely utilized in polymer additive manufacturing. The FDM technology approach is remarkably simple to use and set up in comparison with other AM technologies [7]. FDM is based on melting plastic filaments [8]. The FDM process is performed by extruding thermoplastic material, which has to be heated up to its melting point through a nozzle, then depositing the extruded layers of materials on top of each other [9]. The parameters of FDM process like raster angle, printing speed, printing orientation, and layer height have a significant influence on print characteristics. In order to determine the qualities of components, researchers studied the impacts of various process parameters on responses [7]. Currently, FDM is considered the most widely used technology of all types of 3D Printing techniques due to its low cost of printer devices, simplicity, and variety of inexpensive filaments [10, 11]. FDM 3D printers are commonly applied in different industries like aeronautics, construction, automotive, and medicine for rapid prototyping. Various thermoplastic polymers like acrylonitrile butadiene styrene (ABS), polylactic acid (PLA), and polyimide are used as the material of FDM technology in the shape of filament. ABS material has better elongation, ductility, and flexural strength than PLA material, but it emits an undesired smell in the printing process. On the other hand, PLA material is more environmentally friendly than ABS material because it degrades faster than ABS material and is produced from renewable resources [12].

Simultaneously, lightweight sandwich structures are being used in many industries such as automotive, sustainable energy, and building due to their effect on improving mechanical properties [13]. The frequent use in engineering applications of lightweight sandwich structures shows better results in acceleration, lower fuel and consumption (for aircraft), in addition, to lower life cycle costs due to lower operation costs for many applications. However, the

traditional methods of manufacturing and structures include many stages that require the purchase of complex devices, which is usually difficult to use and make production expensive. Meanwhile, current processes in AM techniques offer great freedom for both realising and designing honeycomb structures with complex geometries. Because of that, a vast number of studies have been carried out to explore the correlations between specific mechanical properties and 3D-printed complex geometries [14-16]. Furthermore, recent research is focused on numerical analysis and geometric design, showing that geometric shape plays a crucial role in their mechanical response [15, 17, 18]. In addition, researchers [19] have been focused their studies on understanding the effect of different sandwich structures (triangle, square, and hexagon shapes) by considering numerous parameters such as the number of infill shapes, nature of the core shape, the orientation of cores, and the influence dynamic behaviour of sandwich structures.

Mechanical performance (bending, compressive, tensile, etc.) of sandwich structures (e.g., honeycomb and rhombus) correlates not only with structure geometry but is also strongly dependent on material properties [20-22]. An initial investigation on the manufacture and testing of mechanical performance (tensile and bending) of honeycomb core sandwich structures printed with different materials (PLA and ABS) and using different filling techniques [23, 24]. PLA is one of the most common materials used in thermoplastic FDM feedstock, which has good printability due to its crystalline phase at room temperature [25]. Also, PLA has excellent mechanical qualities and because of its biodegradability, can be used to replace petroleum-based polymers. The usage of PLA has significantly increased during the past ten years, mostly in the fields of biomedicine and packaging [26, 27]. A unique generation of green composites, or composite materials that are friendly to the environment, may be created with the aid of PLA. Furthermore, PLA is increasingly used in a number of components of composite sandwiches, including adhesion nonwovens, 3D-printed honeycombs, and skins on various composite panel configurations [28]. Additionaly, the potential of PLA-derived materials for use in automotive components has been proved by Nickels [29]. Researchers [30] have also focused their studies on estimating the modal parameters and the properties of damping through experimental dynamic analysis for PLA. However, limited studies have focused on using PLA material in the 3D printing of sandwich structures which could enhance its mechanical behaviour [31, 32].

In this study, the rhombus and honeycomb structures were designed and manufactured with PLA material by FDM printing technology. The material's mechanical performance in the case of sandwich structures was evaluated by conducting mechanical tests (tensile, three-point bending, and compression). The failure mode of specimens for each testing carried out was also analysed and highlighted. However, the static analysis was only investigated in the present work. The outcome of this study could be helpful in examining the capability of PLA sandwich structure to create lightweight materials with equitable mechanical

properties and most importantly to support sustainable development. This will contribute to filling the gap in knowledge regarding the performance of sandwich structures desired in such applications because of their light weight and reliability.

2 Materials and Methods

2.1 Constructing of Sandwich Structure Specimens

The FDM technique was used to manufacture the test specimens with the commercial 3D printer WANHAO Duplicator 6 and PLA (polylactic acid) material. PLA was chosen as the preferred material because of its growing popularity in FDM printing and its sustainable environmental characteristics. The filament used was 1.75 mm in diameter and black in colour. As stated by the manufacturer, the filament's claimed qualities are tensile Young's modulus, ultimate tensile strength, strain at yield, and impact strength of 3.120 GPa, 70 MPa, 5%, and 3.4 KJ/m2, respectively, when tested according to ISO 527. WANHAO 3D printer has a 0.4 mm nozzle diameter and exists in the additive manufacturing laboratory at MATE (Szent Istvan University formerly), Gödöllő, Hungary. The test samples were printed with an infill density of 100% and a layer thickness of 200 µm at a print speed of 60 mm/s. The printing and building plate temperatures were set as 210 ℃ and 60 ℃, respectively.

Sandwiches typically consist of two skins (outer surfaces) and a core (inner structure). The core's material may be the same or unlike the skins. In the current study, the material utilised for both outer surfaces and inner structure was the same (PLA), and the manufacturing, by 3D printing, was done in solely a single stage. Two sandwich structures, honeycomb and rhombus (see Figure 1) have been used. These structures were designed in accordance with the standards ASTM C393 and MIL-STD-401B. A three-dimensional designing software SOLIDWORKS 2016 was used to generate the 3D structure model of the samples and convert it into an "STL" file format. In order to slice the STL file (3D model), Ultimaker Cura 4.7 software was employed. The Cura program translates the digital model into a set of instructions (G-code) for the 3D printer, and through this software, the manufacturing parameters are established. The designed specimens, with the honeycomb and rhombus sandwich structures, were prepared for the tensile, bending, and compression testing, as shown in Figure 1a, Figure 1b, and Figure 1c, consecutively. Magnification for the sandwich structures' core shape is aside demonstrated in Figure 1: honeycomb core (left) and rhombus core (right). The specimens were built at an on-edge orientation, as illustrated in Figure 2d.

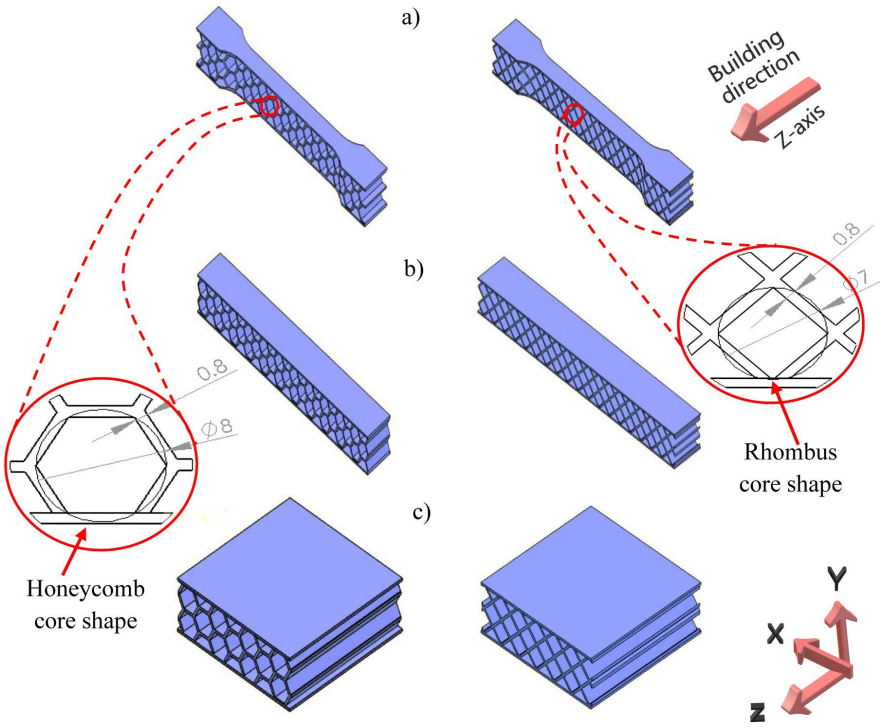

Figure 1
3D models of the sandwich structure specimens of the honeycomb (left) and rhombus (right) patterns for a) tensile test, b) three-point bending test, and c) compression test

According to the appointed standards, the tensile and three-point bending test specimens have the dimensions of 150 mm, 20 mm, and 15 mm for length, width, and height, respectively, with 0.75 mm as the thickness of the skin (see Figure 2a-b). Also, the compression test samples were designed with a length of 50 mm, a width of 50 mm, and a height of 15 mm, at a skin thickness of 0.75 mm (see Figure 2c). Three identical specimens were 3D-printed for each test condition. The cell wall thickness should be sufficient so that it can be easily printable by the FDM machine since too thin a cell wall thickness might make printing difficult and can deform the object. Therefore, the proper cell size was chosen to make the cell wall thickness thick enough to be easily printed. The chosen cell sizes were 8 mm and 7 mm for the honeycomb and rhombus, respectively. In addition, the cell wall size for both the honeycomb and rhombus was 0.8 mm (see core shape aside in Figure 1). However, it is worth noting that it is not easy to specify the accurate or optimal 3D printing parameters due to the anisotropic nature caused by the technology owing to the variety of its printers and materials [33]. Figure 2d shows the actual appearance of some of the manufactured samples. The tensile specimens were produced with structure support owing to their geometry as there

is a wide space under their gauge section. However, there was no need for structural support while creating the bending and compression test pieces. The average density values for the specimens examined are tabulated in Table 1.

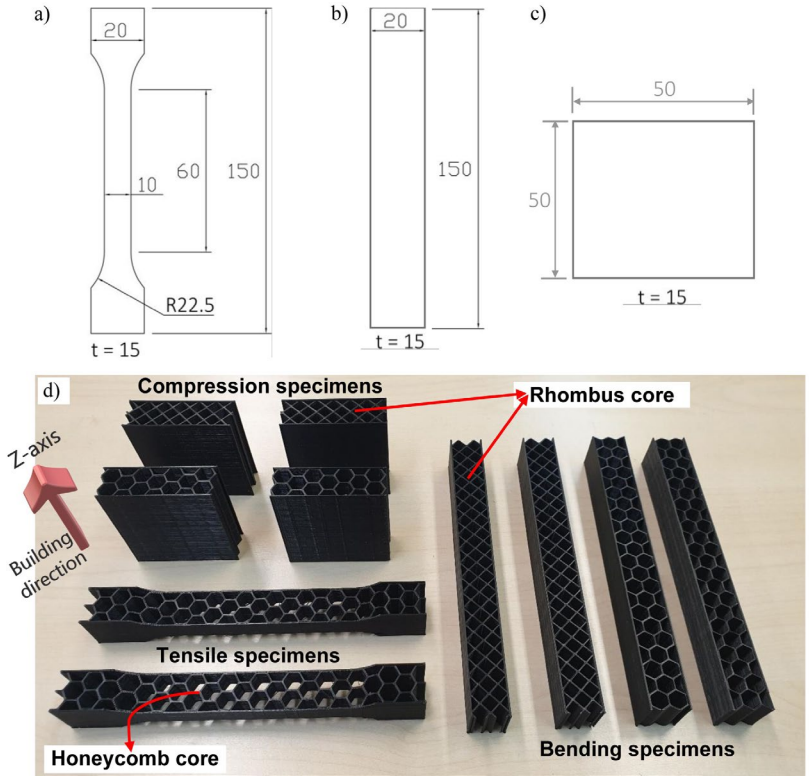

Figure 2
Specimens' dimensions of a) tensile test, b) bending test, c) compression test; and d) physical appearance of some of the test specimens after 3D printing

Table 1
Average values of mass and density (with its standard deviation (SD)) of specimens tested

Structure	Mass (g)	Volume (mm^3)	Density (g/mm^3)	SD (±)
Tensile honeycomb	10.408	31500	$0.33*10^{-3}$	$6.73*10^{-6}$
Tensile rhombus	11.639	31500	$0.369*10^{-3}$	$4.93*10^{-7}$
Bend. honeycomb	14.955	45000	$0.332*10^{-3}$	$1.47*10^{-6}$
Bend. rhombus	17.228	45000	$0.382*10^{-3}$	$2.56*10^{-6}$
Comp. honeycomb	12.063	37500	$0.321*10^{-3}$	$1.22*10^{-6}$
Comp. rhombus	14.533	37500	$0.387*10^{-3}$	$1.15*10^{-6}$

2.2 Experimentations

The universal test machine (Zwick / Roell Z100, Germany) was used to test sandwich structure specimens for compression, tensile, and three-point bending. Three repeated tests have been accomplished on the samples that were constructed for each configuration of the sandwich structure's core (honeycomb and rhombus). The following sections clarify the conditions and details of the tests performed.

2.2.1 Tensile Testing

The ISO standard 527 for tensile testing of polymers [34] was used to assess the tensile properties of the built structures. The tensile behaviour determination included the tensile strength, tensile Young's modulus, and the failure form under the specified conditions. According to the ISO 527-2:2012 standard [35], the specimens were stretched at a steady speed of 1 mm/min along their main axis until they broke (Figure 3).

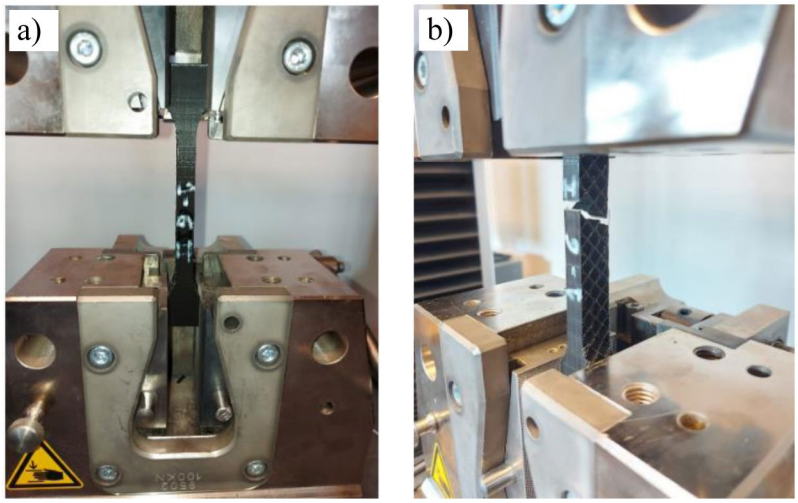

Figure 3
Tensile testing for one of the sandwich structure's specimens (rhombus), a) during the test and b) after breakage

Equation (1) was used to calculate the tensile strength (σ_t) of sandwich specimens

$$\sigma_t = P_t / A_t \,, \tag{1}$$

where P_t stands for the ultimate load (N), while the sandwich specimen's cross-sectional area is represented by A_t (mm^2). In this study, the broken cross-section was chosen to calculate the tensile cross-sectional area, where it was assumed to be the weakest point (having the smallest cross-sectional area) within the gauge

section of the specimens. For this, the Solidworks software was used to find and calculate the smallest cross-sectional area, as illustrated in Figure 4, where it was 30 mm^2 and 32 mm^2 for honeycomb and rhombus, respectively.

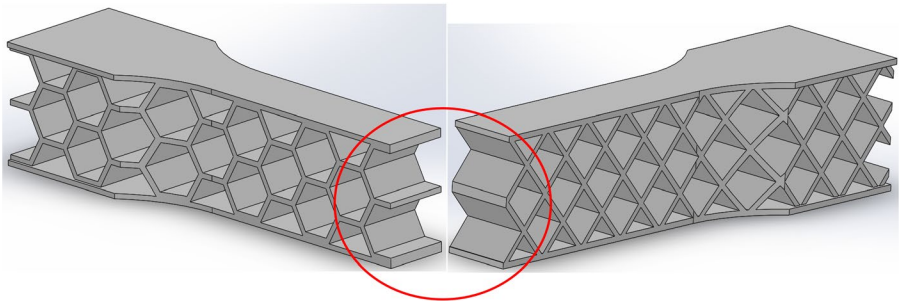

Figure 4
The cross-sectional area of tensile specimens determined by the Solidworks software

Tensile modulus (E_t) was calculated by Hooke's law

$$E_t = \sigma_t/\varepsilon \,, \tag{2}$$

as ε is the strain.

To get a more accurate value of Young's modulus (E_t), two points were fitted on the stress-strain curves of the sandwich specimens to draw the slope and determine the tensile modulus. These two points were specifically at 10% and 60% from each axis on the stress-strain curve (i.e., the values of σ_t and ε were picked at 10% and 60% and then substituted into the slop equation; $\sigma_{t(\text{at } 60\%)} - \sigma_{t\ (\text{at } 10\%)} / \varepsilon_{(\text{at } 60\%)} - \varepsilon_{(\text{at } 10\%)}$.

2.2.2 Bending Testing

The bending tests (three-points) were carried out in accordance with ASTM C 393 [36]. The crosshead speed of the tests was 1 mm/min until the specimen broke. In the three-point bending, the radius of supports and punch was 15 mm, and the span length was 100 mm. Equations (3) and (4) were used to calculate the values of bending strength (σ_b) as well as the bending modulus (E_b) of sandwich samples [37]

$$\sigma_b = (3P.s)/(2b.d^2) \,, \tag{3}$$

$$E_b = (s^3.m)/(4b.d^3) \,, \tag{4}$$

where P stands for the force (N) at a particular point on the load-deflection curve, while s is the support span length (mm), in addition, b and d are the width (mm) and thickness (mm) of the sandwich specimen, respectively. Also, the tangent's slope to the load-deflection curve's initial straight-line component (N/mm) is m. The experimental setup of the three-point bending test is shown in Figure 5a.

2.2.3 Compression Testing

The compression of the sandwich structure specimens was carried out on a mechanical test machine (Figure 5b). The tests were performed at a 1 mm/min crosshead speed. For reliable results, each lightweight sandwich construction investigated (honeycomb and rhombus) was subjected to three tests.

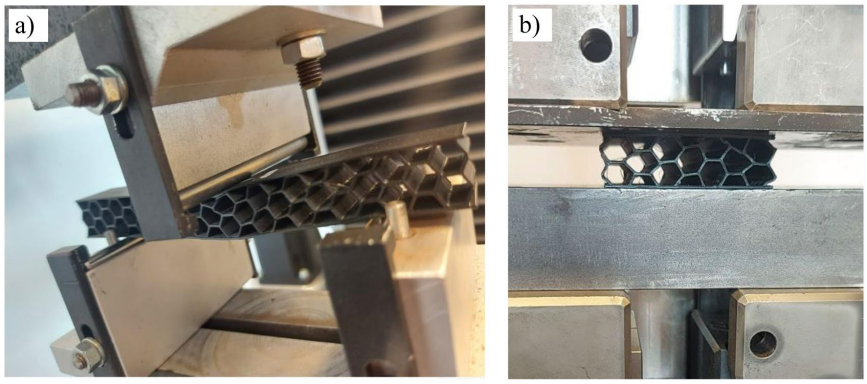

Figure 5
Experimental setup of testing one of the sandwich structures (honeycomb) for the tests of a) three-point bending and b) compression

The compressive strength (σ_c) value of the sandwich specimens was calculated using Equation (5)

$$\sigma_c = P_c / A_c, \tag{5}$$

where P_c represents the ultimate load (N) on the compression tests, and A_c is the sandwich specimens' cross-sectional area (mm^2).

Equation (6) was used to determine the compressive modulus (E_c)

$$E_c = (m.t)/A_c, \tag{6}$$

where m is the tangent's slope to the load-deflection curve's initial straight-line component (N/mm) and t denotes the core thickness (mm).

In order to calculate the cross-sectional area of the compression samples, and based on a solid structure, the average area (A_{av}) of the structure can be determined as follows, $A_{av} = V_{str}/t$ where V_{str} represents volume of sandwich structure and t is the thickness.

Since density (ρ) is the mass (M) over volume (V), thus,

$$\rho_{av} = M_{str}/V, \tag{7}$$

and

$\rho_{pla}=M_{pla}/V \rightarrow$

$V= M_{pla}/\rho_{pla}$, (8)

where ρ_{av} and M_{str} denote the density and mass, respectively, of the core sandwich structure. Meanwhile, ρ_{pla} and M_{pla} are the density and mass of a solid structure for PLA polymer.

Substituting Eq (8) in Eq (7),

$\rho_{av}=(M_{str}/M_{pla})\times\rho_{pla} \rightarrow$

$M_{str}=(\rho_{av}/\rho_{pla})\times M_{pla}$ (9)

$\because V_{str}=A_{av}.t$, and $\rho_{pla}=M_{str}/V_{str}$,

$\therefore \rho_{pla}=M_{str}/(A_{av}.t) \rightarrow$

$A_{av}=M_{str}/(\rho_{pla}.t)$ (10)

Putting (9) in (10),

$A_{av}=(M_{pla}/\rho_{pla}.t)\times(\rho_{av}/\rho_{pla})$ (11)

$\because \rho_{pla}=M_{pla}/(A_{pla}.t)$

$\therefore A_{pla}=M_{pla}/(\rho_{pla}.t)$ (12)

From (11) and (12),

$A_{av}= A_{pla}\times(\rho_{av}/\rho_{pla})$ (13)

The density (ρ_{av}) of the sandwich structure compression specimens is $0.32*10^{-3}$ (g/mm^3) for honeycomb and $0.39*10^{-3}$ (g/mm^3) for rhombus, as listed in Table 1. Additionally, the density of the PLA material (ρ_{pla}), in case of a solid bulk, is $1.252*10^{-3}$ (g/mm^3).

3 Results and Discussion

3.1 Tensile Performance of Sandwich Structures

Figure 6a shows the load-displacement curves that were obtained from the tensile test of the honeycomb and rhombus sandwich structures. Obviously, the rhombus core sandwich samples had the greatest maximum load of 714 N in the load-elongation curves. In terms of the tensile strength, which ranged between 19.49 and 23.01 MPa, the better values were from rhombus core sandwich structures

(see Figure 6b). The increased tensile strength of these specimens is due to their reliable core structure, which had more contact sites at the fracture area under tensile stress than the honeycomb core construction (see Figure 7). Therefore, the applied load was distributed across a larger area, resulting in higher resistance to failure. In contrast, honeycomb sandwich structures had the best tensile Young's modulus of 599 MPa compared to rhombus (440 MPa), as shown in Figure 6c. Zaharia et al. [38] have studied the mechanical properties of different sandwich structures (honeycomb, diamond-celled (resembles the rhombus in the current work), and corrugated). They reported a higher load (required to fracture) and tensile strength for the diamond structure than the honeycomb, which is in good agreement with the present study findings.

Figure 7 shows that sandwich specimens seem to be failed first due to the yielding of the face sheet (shell), thereafter the core (inner structure) shear failure. One of the outer surfaces of the sandwich specimens yielded, the fracture progressed through the whole core, and finally terminated at the lower level, causing cracking of the other outer surface. The specimens, as shown in Figures 7a and 7b, had a complete fracture of the whole structure, beginning with the first outer surface (shell), then the core, and lastly the second outer surface, for both (honeycomb and rhombus) tested sandwich structures.

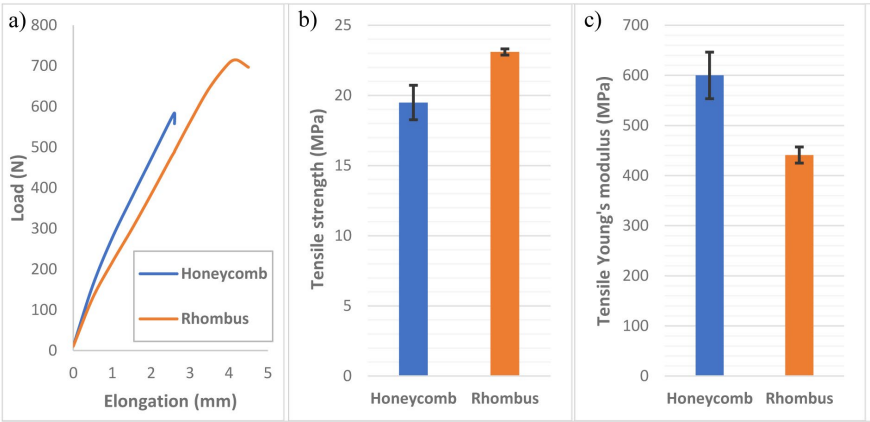

Figure 6
Tensile test result of sandwiches structure specimens, a) load-displacement curves, b) tensile strength values, and c) Young's modulus values

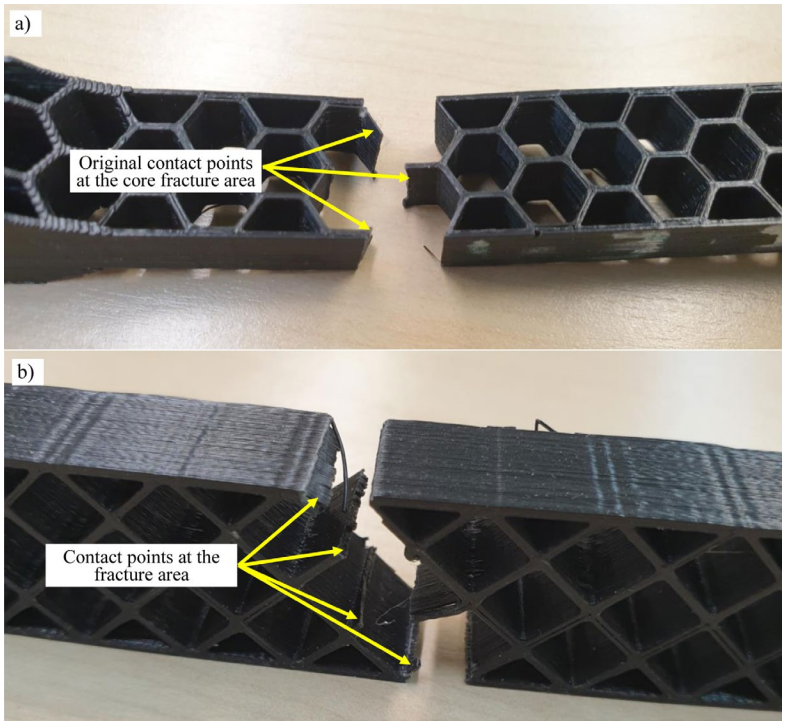

Figure 7
Fracture shape and contact sites at the core structure failure area after the tensile tests of a) honeycomb, and b) rhombus sandwich specimens

3.2 Three-Point Bending Performance of Sandwich Specimens

The flexural performance of the lightweight sandwich constructions (honeycomb and rhombus), including bending strength, bending modulus, and stress-displacement characteristics, was investigated using this test approach. The load-displacement curves of test specimens for three-point bending have two main stages, as shown in Figure 8a: a steady increase between the load applied and the displacement towards the curve's maximum, but then when the specimens broke, there was a sudden decline from the maximum load. Sugiyama et al. [15] attributed this non-linearity or sharp decline exhibited in the load curve to the gradual failure progression. They mentioned that in the fracture mode, the crack initially happens at the upper skin while wrinkling occurs at the core, causing the curve to drop. Using Equations (3) and (4) and the sandwich specimen dimensions, the test machine software automatically determined the bending modulus and bending strength, which are the most essential three-point bending aspects.

Three-point bending results were better for the rhombus than the honeycomb core sandwich structure. The maximum force reported was about 381 N at a displacement of 4.47 mm of rhombus core specimens, according to the curves shown. In terms of the bending strength, Figure 8b exhibits that the rhombus core sandwich models had a bending strength average value of 40% higher than that of the honeycomb core sandwich samples. Furthermore, the bending Young's modulus of rhombus specimens was twice as high as that of honeycomb specimens (see Figure 8c).

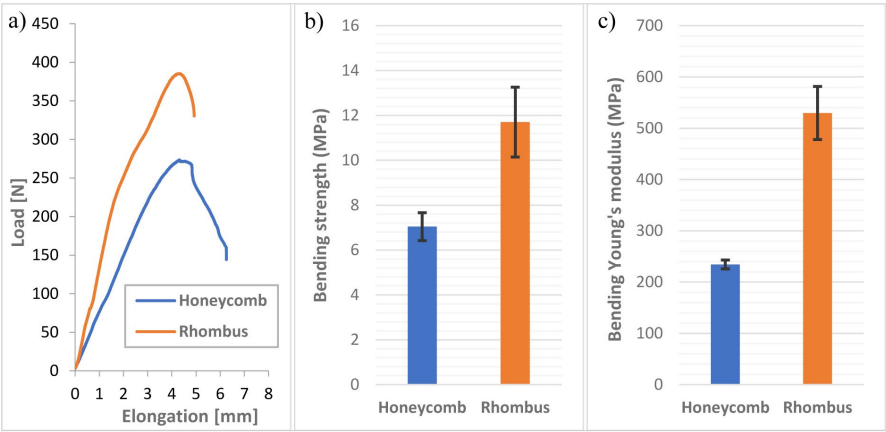

Figure 8
Three-point bending test results of sandwich structures, a) load-displacement curves, b) bending strength, c) Young's modulus of bending

The primary failure scenarios of sandwich structures that occurred during three-point bending tests are shown in Figure 9. The fracture point pictured in Fig. 9a was not at the same loading point while testing. This is due to, at the fracture site, the core being at an angle perpendicular to the longitudinal axis, making fracture/buckling easy [15]. Sandwich specimens with thin skins may readily fail in a skin yield mode because rhombus core sandwich faces/skins practically withstand all tensile and compressive loads in bending [38]. However, an indentation mode occurs initially when the core sandwich walls are thick enough, but given sufficient impact energy, the sandwich structures will eventually collapse in a skin yield fracture mode on the top face [39]. Then, cracks are formed in the rhombus core, followed by propagation of the failure up to the lower face. On the other hand, the bending test results of the honeycomb core structure specimen showed that a tension failure in the upper skin takes place like compression face buckling/wrinkling (see Figure 9b). Local short-wavelength wrinkling of skins is another name for this sort of failure mechanism [40].

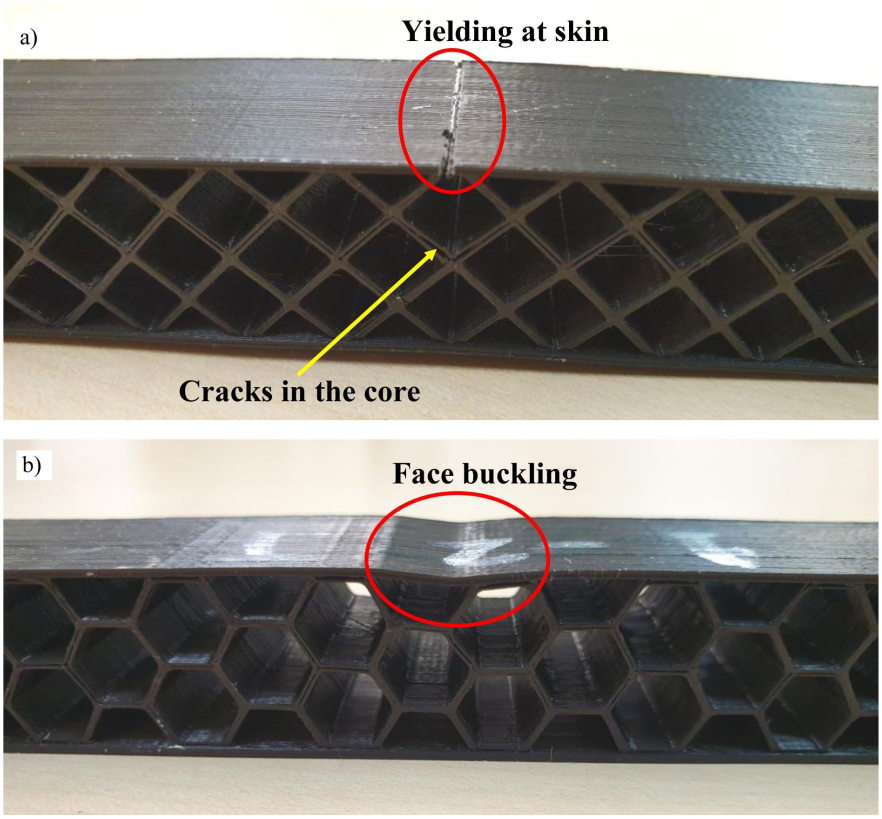

Figure 9
Three-point bending test's failure modes of sandwich specimens; a) rhombus, and b) honeycomb core structures

3.3 Compression Behaviour of Sandwich Structures

The present section discusses the compression test results obtained for 3D-printed rhombus and honeycomb structure specimens. Figure 10 exhibits the compression behaviour gained from the compression tests for each examined type of sandwich structure. It is evident from Figure 10a that the load-displacement responses are generally linear until the core shear starts, at which point there is a dramatic reduction in load. The maximum force (roughly 5850 N) was found in the rhombus core structures (at an elongation of 1.6 mm) until unredeemable damage in this sandwich structure had occurred. However, for the honeycomb structure, irreversible damage occurred when the load force reached 2820 N at 1.35 mm elongation.

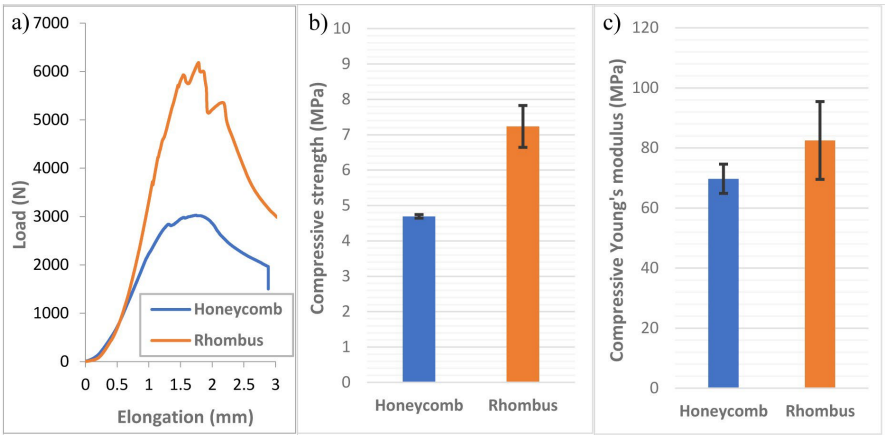

Figure 10
Compression test results, a) load-elongation curves, b) compressive strength, and c) Young's modulus of compression

The results of compressive stress and modulus are represented in Figure 10b and Figure 10c, respectively. The cross-section area was calculated using Equation (13), as mentioned in section 2.2.3.

Again, the rhombus core sandwich structure offered the best performance as the average of its compressive strength (7.23 MPa) was 35.1% higher than that of the honeycomb (4.69 MPa) and its compressive modulus (82.47 MPa) was 15.4% better than the honeycomb (69.73 MPa). The dense network of its structures, which also caused these specimens to weigh more (as shown in Table 1), is responsible for the outstanding performance of rhombus core specimens.

Figure 11 shows the specimens after the compression. For the honeycomb specimen (Figure 11a), deformations develop in the structure's core as the breakdown was the buckling and then shearing of the core of the sandwich. This may be explained by the fact that when sandwich structures are compressed, the skins are too thick and robust to be crushed, resulting in a core buckling failure mode. However, in the case of rhombus structure (Figure 11b), the extruded filament layers were debonded because the sandwich's core had a high degree of flexibility.

Comparing Figures 6 and 10, it can be noticed that the tensile Young's modulus (E_t) is much higher (almost 8 times for honeycomb and 5 times for rhombus) than the compressive modulus (E_c). This significate difference in the magnitudes can be attributed to the influence of test load direction with respect to the sandwich structure. In the case of tensile, the load is parallel to the sandwich structure, and the shell (the outer skins) can support the core structure significantly to provide much more strength. However, for the compression, and due to the loading direction as well, the whole load will be applied on the core sandwich structure,

causing failure in it without any support from the outer shells, as shown in Fig. 11, as the skins were not affected. This would make the specimen's compressive strength, and implicitly the compression modulus, much weaker than the tensile ones.

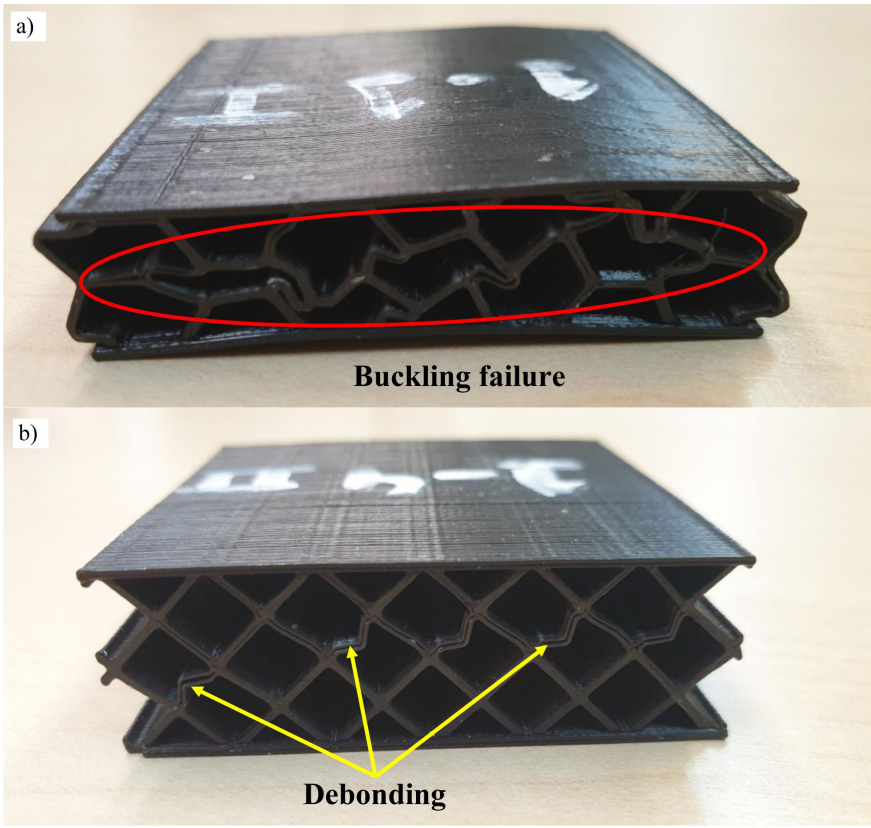

Figure 11

Failures mode of the sandwich specimens after the compression, a) core shearing for the honeycomb sandwich structure, and b) debonding of the extruded filament layers for the rhombus specimens

Conclusions

In the current study, the manufacture and characterisation of 3D-printed two different sandwich structures (honeycomb and rhombus) were executed. At first, using the fused deposition modelling technique, PLA filament was employed to prepare tensile, three-point bending, and compression testing specimens. Then, the characteristics of the sandwich structures fabricated of PLA material were studied based on the tests carried out. It was observed that the rhombus sandwich samples demonstrated the best tensile strength (23.01 MPa), which was 15.3% higher than the honeycomb, due to their reliable core structure. Furthermore, rhombus

specimens exhibited the maximum compression strength (7.23 MPa) and flexural strength (11.7 MPa), 35.1% and 39.8%, respectively, higher than the honeycomb. It was noticed that 3D-printed sandwich structural collapse is primarily due to the failure of the core. In the fields of biomedicine and packaging, lightweight sandwich structures are widely utilised to lower the total weight of mechanical components. Therefore, the findings of this work are proposed to provide the industry of these applications with some useful data.

Acknowledgement

This work was supported by the Stipendium Hungaricum Programme and by the Mechanical Engineering Doctoral School, Szent István Campus, MATE University, Gödöllő, Hungary.

References

[1] Erdős F., Németh R., "AMT-based real-time, inter-cognitive communication model", Acta Polytechnica Hungarica, Vol. 16, No. 6, pp. 115-127, 2019

[2] Rafajłowicz E., "Data Structures for Pattern and Image Recognition and Application to Quality Control", Acta Polytechnica Hungarica, Vol. 15, No. 4, pp. 233-262, 2018

[3] Hanon M. M., Zsidai L., "Sliding surface structure comparison of 3D printed polymers using FDM and DLP technologies", IOP Conference Series: Materials Science and Engineering, Vol. 749, pp. 012015, 2020

[4] Antony S., Cherouat A., Montay G., "Fabrication and Characterization of Hemp Fibre Based 3D Printed Honeycomb Sandwich Structure by FDM Process", Applied Composite Materials, Vol. 27, No. 6, pp. 935-953, 2020

[5] Chaczko Z., Klempous R., Rozenblit J., Adegbija T., Chiu C., Kluwak K., Smutnick C., "Biomimetic Middleware Design Principles for IoT Infrastructures", Acta Polytechnica Hungarica, Vol. 17, No. 5, pp. 135-150, 2020

[6] Hanon M. M., Ghaly A., Zsidai L., Szakál Z., Szabó I., Kátai L., "Investigations of the Mechanical Properties of DLP 3D Printed Graphene/Resin Composites", Acta Polytechnica Hungarica, Vol. 18, No. 8, pp. 143-161, 2021

[7] Alzyod H., Ficzere P., "The Influence of the Layer Orientation on Ultimate Tensile Strength of 3D Printed Poly-lactic Acid", JJMIE, Vol. 16, No. 3, 2022

[8] N. Turner B., Strong R., A. Gold S., "A review of melt extrusion additive manufacturing processes: I. Process design and modeling", Rapid Prototyping Journal, Vol. 20, No. 3, pp. 192-204, 2014

[9] Kun K., "Reconstruction and Development of a 3D Printer Using FDM Technology", Procedia Engineering, Vol. 149, pp. 203-211, 2016

[10] Hanon M. M., Zsidai L., "Comprehending the role of process parameters and filament color on the structure and tribological performance of 3D printed PLA", Journal of Materials Research and Technology, Vol. 15, pp. 647-660, 2021

[11] Liu Z., Wang Y., Wu B., Cui C., Guo Y., Yan C., "A critical review of fused deposition modeling 3D printing technology in manufacturing polylactic acid parts", The International Journal of Advanced Manufacturing Technology, Vol. 102, No. 9-12, pp. 2877-2889, 2019

[12] Ngo T. D., Kashani A., Imbalzano G., Nguyen K. T. Q., Hui D., "Additive manufacturing (3D printing): A review of materials, methods, applications and challenges", Composites Part B: Engineering, Vol. 143, No. December 2017, pp. 172-196, 2018

[13] Dobos J., Hanon M. M., Oldal I., "Effect of infill density and pattern on the specific load capacity of FDM 3D-printed PLA multi-layer sandwich", Journal of Polymer Engineering, Vol. 42, No. 2, pp. 118-128, 2022

[14] Askarinejad S., Rahbar N., "Toughening mechanisms in bioinspired multilayered materials", Journal of The Royal Society Interface, Vol. 12, No. 102, pp. 20140855, 2015

[15] Sugiyama K., Matsuzaki R., Ueda M., Todoroki A., Hirano Y., "3D printing of composite sandwich structures using continuous carbon fiber and fiber tension", Composites Part A: Applied Science and Manufacturing, Vol. 113, pp. 114-121, 2018

[16] Yazdani Sarvestani H., Akbarzadeh A. H., Niknam H., Hermenean K., "3D printed architected polymeric sandwich panels: Energy absorption and structural performance", Composite Structures, Vol. 200, pp. 886-909, 2018

[17] Askarinejad S., Choshali H. A., Flavin C., Rahbar N., "Effects of tablet waviness on the mechanical response of architected multilayered materials: Modeling and experiment", Composite Structures, Vol. 195, pp. 118-125, 2018

[18] Abueidda D. W., Elhebeary M., Shiang C.-S. (Andrew), Pang S., Abu Al-Rub R. K., Jasiuk I. M., "Mechanical properties of 3D printed polymeric Gyroid cellular structures: Experimental and finite element study", Materials & Design, Vol. 165, pp. 107597, 2019

[19] Rajpal R., K. P L., Gangadharan K. V., "Parametric studies on bending stiffness and damping ratio of Sandwich structures", Additive Manufacturing, Vol. 22, pp. 583-591, 2018

[20] Wang X., Jiang M., Zhou Z., Gou J., Hui D., "3D printing of polymer matrix composites: A review and prospective", Composites Part B: Engineering, Vol. 110, pp. 442-458, 2017

[21] Stepashkin A. A., Chukov D. I., Senatov F. S., Salimon A. I., Korsunsky A. M., Kaloshkin S. D., "3D-printed PEEK-carbon fiber (CF) composites: Structure and thermal properties", Composites Science and Technology, Vol. 164, pp. 319-326, 2018

[22] Liu W., Wu N., Pochiraju K., "Shape recovery characteristics of SiC/C/PLA composite filaments and 3D printed parts", Composites Part A: Applied Science and Manufacturing, Vol. 108, pp. 1-11, 2018

[23] Brischetto S., Ferro C. G., Torre R., Maggiore P., "3D FDM production and mechanical behavior of polymeric sandwich specimens embedding classical and honeycomb cores", Curved and Layered Structures, Vol. 5, No. 1, pp. 80-94, 2018

[24] Saad N. A., Sabah A., "An investigation of new design of light weight structure of (ABS/PLA) by using of three dimensions printing", Proceedings of the 13th International Conference "Standardization, Prototypes and Quality: A Means of Balkan Countries' Collaboration", Brasov, Romania. pp. 3-4 (2016)

[25] Zhang P., Arceneaux D. J., Khattab A., "Mechanical properties of 3D printed polycaprolactone honeycomb structure", Journal of Applied Polymer Science, Vol. 135, No. 12, pp. 46018, 2018

[26] Arrieta M., Díez García A., López D., Fiori S., Peponi L., "Antioxidant Bilayers Based on PHBV and Plasticized Electrospun PLA-PHB Fibers Encapsulating Catechin", Nanomaterials, Vol. 9, No. 3, pp. 346, 2019

[27] Oladapo B. I., Daniyan I. A., Ikumapayi O. M., Malachi O. B., Malachi I. O., "Microanalysis of hybrid characterization of PLA/cHA polymer scaffolds for bone regeneration", Polymer Testing, Vol. 83, pp. 106341, 2020

[28] Azzouz L., Chen Y., Zarrelli M., Pearce J. M., Mitchell L., Ren G., Grasso M., "Mechanical properties of 3-D printed truss-like lattice biopolymer non-stochastic structures for sandwich panels with natural fibre composite skins", Composite Structures, Vol. 213, pp. 220-230, 2019

[29] Nickels L., "Car with a biodegradable core", Reinforced Plastics, Vol. 61, No. 6, pp. 332-334, 2017

[30] Ficzere P., Borbás L., "Experimental dynamical analysis of specimens' material properties manufactured by additive technologies", Materials Today: Proceedings, Vol. 12, pp. 352-357, 2019

[31] Lubombo C., Huneault M. A., "Effect of infill patterns on the mechanical performance of lightweight 3D-printed cellular PLA parts", Materials Today Communications, Vol. 17, pp. 214-228, 2018

[32] Zhao H., Li L., Ding S., Liu C., Ai J., "Effect of porous structure and pore size on mechanical strength of 3D-printed comby scaffolds", Materials Letters, Vol. 223, pp. 21-24, 2018

[33] Ficzere P., Lukacs N. L., Borbas L., "The Investigation of Interlaminar Failures Caused by Production Parameters in Case of Additive Manufactured Polymers", Polymers, Vol. 13, No. 4, pp. 556, 2021

[34] International Organization for Standardization, ISO 527-1:2012 - Plastics -- Determination of tensile properties -- Part 1: General principles (2012)

[35] International Organization for Standardization, ISO 527-2:2012: Plastics - Determination of tensile properties - Part 2: Test conditions for moulding and extrusion plastics (2012)

[36] Standard A., "ASTM C393-06. Standard test method for core shear properties of sandwich constructions by beam flexure", ASTM international, pp. 1-7, 2006

[37] Zaharia S. M., Pop M. A., Udroiu R., "Reliability and Lifetime Assessment of Glider Wing's Composite Spar through Accelerated Fatigue Life Testing", Materials, Vol. 13, No. 10, pp. 2310, 2020

[38] Zaharia S. M., Enescu L. A., Pop M. A., "Mechanical Performances of Lightweight Sandwich Structures Produced by Material Extrusion-Based Additive Manufacturing", Polymers, Vol. 12, No. 8, pp. 1740, 2020

[39] Yu J., Wang E., Li J., Zheng Z., "Static and low-velocity impact behavior of sandwich beams with closed-cell aluminum-foam core in three-point bending", International Journal of Impact Engineering, Vol. 35, No. 8, pp. 885-894, 2008

[40] Samali B., Nemati S., Sharafi P., Tahmoorian F., Sanati F., "Structural Performance of Polyurethane Foam-Filled Building Composite Panels: A State-Of-The-Art", Journal of Composites Science, Vol. 3, No. 2, pp. 40, 2019